Illumination Chromaticity Estimation Based on Dichromatic Reflection Model and Imperfect Segmentation

Johji Tajima

Nagoya City University, Yamanohata, Mizuho, Nagoya 467-8501, Japan
tajima@nsc.nagoya-cu.ac.jp

Abstract. The illumination chromaticity estimation based on the dichromatic reflection model has not been made practicable, since the method needs image segmentation beforehand. However, its two-dimensional model is sufficiently robust, when it is combined with the least square method. The proposed algorithm executes the color space division instead of the segmentation. The original image is divided into small color regions, each of which corresponds to one of color sub-spaces. Though this division is imperfect image segmentation, the illumination chromaticity estimation based on the chromaticity distribution in the color regions is possible. Experimental result shows that this method is also applicable to images of apparently matt surfaces.

Keywords: Illumination color estimation, Dichromatic reflection model, Color space division.

1 Introduction

Illumination color/chromaticity estimation from an image is one of the essential problems in color image processing. Computational color constancy algorithms based on the estimation have been proposed for identification of objects under various illuminations. If illumination color is known, object identification by color information becomes easier. In digital cameras, 'white balancing' is an important function. It estimates the illumination color/chromaticity of the scene in a photographed image; then some other digital process compensates the estimated color shift of the image. Color image simulation under other illumination would also be possible if the illumination color can be estimated.

Conventionally, the "Maximum of RGB (MOR)" algorithm or the "Gray World Assumption (GWA)" algorithm has been used for the illumination estimation in practice. They work reasonably well in normal cases. However, MOR fails if the image does not contain any 'white' object or objects with the maximum RGB values. It is self-evident that the GWA does not hold in many situations. For example, the average color of an image of green leaves is not gray.

Recently, many algorithms have been proposed from the view point of color constancy. The "Color by Correlation" algorithm [1] compares the chromaticity gamut of

A. Trémeau, R. Schettini, and S. Tominaga (Eds.): CCIW 2009, LNCS 5646, pp. 51–61, 2009.

an input image with the illumination color gamut which is filled by possible object colors under the illumination. If any color of the image is outside the illumination color gamut, the image is judged not to have been taken under the illumination. Possible illuminations are estimated in that way.

The pattern recognition approach [2][3] is more straightforward, though the information used is similar to that in the color by correlation algorithm. A chromaticity diagram is divided into many tiny regions. The chromaticity distribution of an image is described as an occupation map of the regions. Considering the maps as feature vectors, the pattern learning process is carried out, using many images. After the learning process, arbitrary images can be classified. Chromaticity estimation performance is reported to be good. The drawback of these algorithms is that the image to be classified must have many colors. As an image with a small number of colors occupies a small area on the chromaticity diagram, its chromaticity distribution could be from under various illuminations; that makes it difficult to limit the range of possible illumination. In addition, the pattern recognition approach needs many images for learning.

This paper deals with the illumination chromaticity estimation method based on the "Dichromatic Reflection Model," with which the estimation is possible, in principle, even if the image has only two colors. However, it has been considered impractical, since the image must be segmented before the estimation process. This paper shows that the method is practical even if the image segmentation is imperfect.

2 Illumination Color Estimation Based on the Dichromatic Reflection Model

Shafer proposed the "Dichromatic Reflection Model (DRM)" for computer vision [4]. The model is simply described by Eq.(1):

$$\begin{pmatrix} R \\ G \\ B \end{pmatrix} = \alpha \begin{pmatrix} R_o \\ G_o \\ B_o \end{pmatrix} + \beta \begin{pmatrix} R_w \\ G_w \\ B_w \end{pmatrix} \tag{1}$$

where $(R_o, G_o, B_o)^t$ is the color of the diffuse reflection (i.e. the object color), and $(R_w, G_w, B_w)^t$ is the color of the specular reflection (i.e. the illumination color). It is known that Eq. (1) holds for almost all non-metal objects [5]. The model means that the observed color values $(R, G, B)^t$ of an object with one homogeneous color are distributed on a plane in the RGB three-dimensional color space.

When there is another object with another homogeneous color $(R'_o, G'_o, B'_o)^t$ in the image, observed color values are distributed on another plane. As the illumination color is common for all objects, two planes intersect at the illumination color vector (Fig.1). Hence the illumination color is estimated as follows.

(1) Calculate the plane on which the color distribution of each object lies.
(2) Estimate the line where the planes intersect as the illumination color vector [6][7].

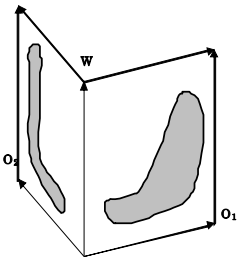

Fig. 1. Illumination estimation based on the Dichromatic Reflection Model

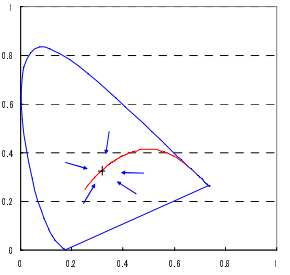

Fig. 2. Chromaticity of dichromatically reflected light lies on straight lines

This algorithm needs only two colors in an image for the estimation. However, this algorithm has not yet come into use, since each color object (or color region on an object) must be segmented before the distribution plane is calculated.

This three-dimensional DRM can be reduced to the two-dimensional model [8]. In color science, it is known that the chromaticity of the mixture of two colored lights is on the straight line that connects the chromaticities of the two colors on the chromaticity diagram. The chromaticity $(x, y)^t$ is calculated by Eq.(2), if the tri-stimulus values are CIE-XYZ values. It is also true for $(r, g)^t$, if the tri-stimulus values are RGB values.

$$x = \frac{X}{X+Y+Z}, \quad y = \frac{Y}{X+Y+Z} \tag{2}$$

This means that $(x, y)^t$ is on the straight line that connects the object chromaticity $(x_o, y_o)^t$ and the illumination chromaticity $(x_w, y_w)^t$. If there are many objects, many lines that are oriented toward the illumination chromaticity should lie on the chromaticity diagram (Fig.2). Detecting the intersection of these lines, we can obtain the illumination chromaticity.

The illumination chromaticity estimation using this two-dimensional model has been studied. Lehmann and Palm [9] applied the model to color lines around specular highlights in an image. This algorithm needs specular highlights in the image. Finlayson and Schaefer [10] discussed the model to estimate the chromaticity of Planckian radiator-like illuminations, assuming the segmentation is perfect. Ebner and Herrmann [11] applied the model to image regions which have been segmented, and whose color saturation is high.

However, though it is necessary for the three-dimensional model to perfectly segment the image and precisely detect the plane, it is expected for the simplified two-dimensional model that the illumination chromaticity estimation by the line detection could be made robust so that the image segmentation might not have to be perfect.

In practical cases, the chromaticity of an object (or a color region) does not exactly lie on a line because of the image noise. For real applications, the following procedure is more reasonable.

(1) Apply the principal component analysis (PCA) to the chromaticity value distribution of the pixels in each color region. Two eigenvalues σ_1 and σ_2 are obtained.
(2) If the relation $\sigma_1 >> \sigma_2$ holds, we assume that the chromaticity values lie on the line which is in the direction of the first principal component.
(3) As the lines are not expected to cross each other at a point in real cases, the chromaticity point with the smallest squared distances from the lines is estimated to be the illumination chromaticity.

The distance d_i between the i-th line (Eq.(3)) and the point (x,y) is expressed by Eq.(4).

$$a_i x + b_i y + c_i = 0 \tag{3}$$

$$d_i = \frac{|a_i x + b_i y + c_i|}{\sqrt{a_i^2 + b_i^2}} \tag{4}$$

The least square method, in which $F(x, y) = \sum_i w_i d_i^2$ is minimized, definitely determines the illumination chromaticity $(x_w, y_w)^t$, where w_i is a weight, which may be the area of the color region, since statistics would be more reliable if the region is larger. The minimization is carried out by solving the simultaneous equations (Eq.(5)).

$$\frac{\partial F(x, y)}{\partial x} = 0, \qquad \frac{\partial F(x, y)}{\partial y} = 0 \tag{5}$$

Now that the illumination chromaticity estimation is formulated on the least squares method, the estimation can be made robust using many color regions, even if each distribution line estimation result is not so reliable because of the image noise.

3 Color Space Division for Imperfect Segmentation

The reason why the illumination color estimation based on DRM has not been developed might be the impression that the color distribution plane can be estimated only when a color region contains a wide-range color variation from the diffuse reflection to the specular reflection. For obtaining such a color region, a very powerful image segmentation technique would be necessary. However, in the previous section, the problem is reduced to the distribution line estimation in the two-dimensional chromaticity space. It is easier to detect a small chromaticity shift, even if the color region is small. For this purpose, we try to use a color image segmentation algorithm that segments an image based on the color information. The algorithm might divide a large color region that contains a wide-range color variation into several small sub-regions, each of which containing only a part of the wide color variation. However, it is sufficient if the sub-region contains a part of chromaticity shift from the object chromaticity $(x_o, y_o)^t$ to the illumination chromaticity $(x_w, y_w)^t$.

The color space division described in this section is a technique to be used to imperfectly segment an image. This technique was originally developed to represent a color image with a small number of colors. Using the algorithm, a full color

(24-bit/pixel) image could be represented by 256 colors without visual degradation [12]. In this application, the algorithm is adjusted so that normal images are represented by about 20~50 colors.

The color space division is carried out in the following steps.

(1) Convert the color space from RGB to CIELAB, and consider the whole three-dimensional space as one color sub-space.

(2) Compute the pixel color distribution in each color sub-space, and apply 'principal component analysis (PCA)'.

(3) Divide the sub-space by a plane that is perpendicular to the first principal axis, so that the new two sub-spaces satisfy the criterion for the discriminant analysis [13]. This division is not carried out when either of the following two conditions is satisfied.

   (a) The color difference between the mean colors of the pixels in the two sub-spaces is smaller than a predetermined threshold (=*th*). *th* is determined so that all colors within the final sub-space may be considered to have the same color.

   (b) The number of pixels in one of the two sub-spaces is smaller than a predetermined threshold (=*n*). This prevents a sub-space being generated by the image noise.

(4) If there is no sub-space that can be divided, finish the division. Otherwise, return to step (2).

The division takes place in the three-dimensional L*-a*-b* color space, and every pixel is classified to one of the sub-spaces. For the explanation purpose, this division is illustrated in the two-dimensional a*-b* color space in Fig.3. A color distribution is illustrated as a contour map.

For the pixel colors in the whole space S_0, the principal axis PC_0 is calculated. The division plane DP_0, which is perpendicular to PC_0, divides S_0 to generate sub-spaces S_1 and S_2. This procedure is repeated for the sub-spaces, and sub-spaces S_{11} and S_{12} are generated from S_1 based on the principal axis PC_1 and the division plane DP_1. S_{21} and S_{22} are generated from S_2 by the same procedure.

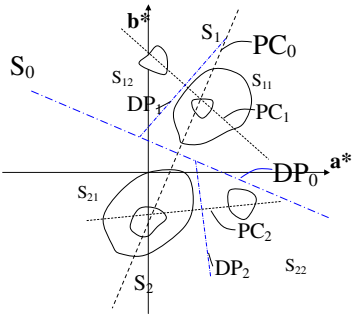

Fig. 3. Color space division

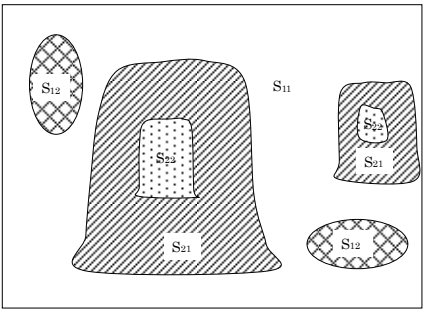

Fig. 4. Color region image. Each region corresponds to the color sub-space.

Though this is the color space division procedure, the color image is also divided into color regions, each of which corresponds to a sub-space (Fig.4). However, multiple color regions in an image may correspond to a single color sub-space. To make sure that the chromaticity distribution of one color region is analyzed, the connected component labeling process is applied to the color region image. By this process, many connected color regions are generated. For these color regions, chromaticity distribution is analyzed.

4 Experiments

4.1 Illumination Chromaticity Estimation

As the first experiment, a scene that contains typical dichromatic reflection objects was processed (Fig.5). Colorful plastic objects are illuminated by fluorescent lamps in a lighting booth (Gretag-Macbeth Judge II®). Figure 5(a) shows the scene under the illuminant D65 simulator (Condition 1). The image was taken by a consumer use

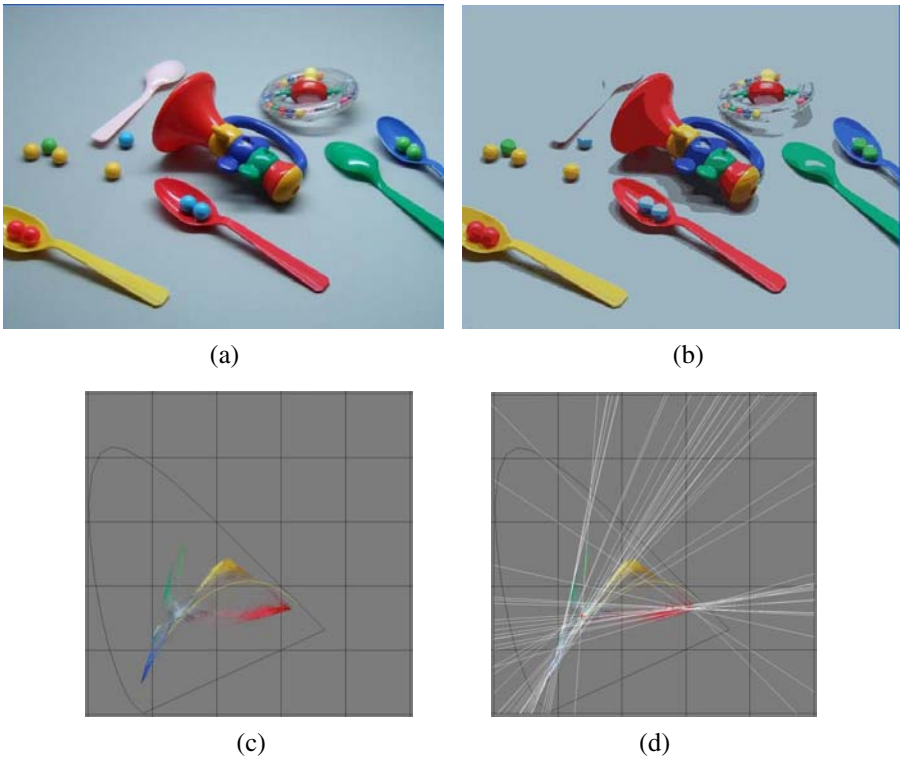

Fig. 5. Experiment on an image with dichromatic objects: (a) Input image under Condition 1. (b) Color region image (54 colors). (c) Chromaticity distribution of reliable pixels. (d) Illumination chromaticity estimation.

digital camera Fujifilm *FinePix F31fd*. The auto white balancing function was off, and the color balance was set to 'Daylight'. Auto exposure control function was used, and specular highlights are included in this image. Image size was reduced to 640×480 pixels. Obtained RGB pixel values are dealt with as sRGB values.

The color space division procedure requires two parameters as described in 3. The parameters *th* and *n* were set to 10 and 256, respectively. For this image, the whole color space was divided into 54 subspaces. After the connected component labeling, the original image was divided into 7297 color regions. The color region image is shown in Fig. 5(b). Large color region with wide color variation (e.g. the red color region in the bell part of the toy trumpet) is divided into four or five color regions, while some color region (e.g. the pink spoon) is united with a neighboring region.

The chromaticity estimation was carried out with reliable pixels in a color region with 'good' characteristics. Four threshold values were defined. Chromaticity calculation is reliable only for the pixels that are neither very dark nor saturated. Hence, chromaticity was calculated for the pixels that satisfies the following conditions: (a) $R+G+B \geq RGB_{\min}$ and (b) $\max(R,G,B) \leq RGB_{\max}$. In these calculations, the linearized *R*, *G* and *B* values (i.e. no original sRGB values) were used. A color region with the 'good' characteristics is a color region in which the number of reliable pixels is sufficiently large and the pixel chromaticities are distributed in a linear shape. The minimum for the number of reliable pixels was defined as n_r. The distribution shape was defined by the *ratio* between the standard deviations σ_1 and σ_2 in two principal axes. These threshold values were temporarily set to $RGB_{\min}$=50, $RGB_{\max}$=240, n_r=200 and *ratio*=2.0, respectively. However, the estimation result was not sensitive to the threshold selection.

Figure 5(c) shows the chromaticity distribution of reliable pixels. On the *x*-*y* chromaticity diagram, blackbody chromaticity locus (yellow) and daylight chromaticity locus (orange) were added. In addition, the first principal axes for 'good' color regions were depicted with white lines in Fig.5 (d), where the estimated illumination chromaticity was shown with a red cross, too. The estimated chromaticity for this

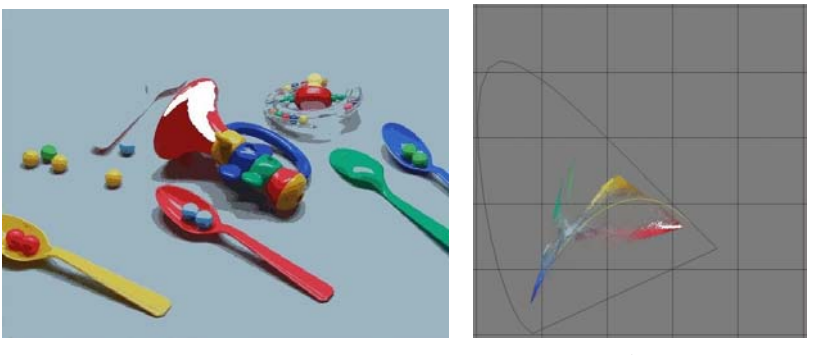

(a) (b)

Fig. 6. Typical chromaticity distribution in a color region. The chromaticity of the color region painted in white in (a) is distributed in the white region in (b).

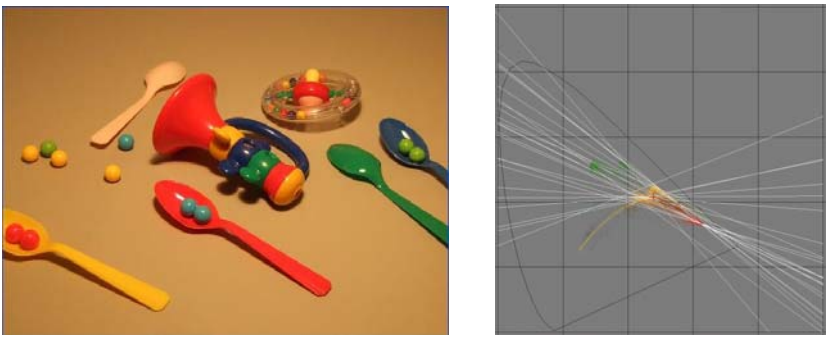

(a) (b)

Fig. 7. Experiment under Condition2: (a) Input image under Condition 2. (b) Illumination chromaticity estimation.

image was (x_1,y_1)=(0.2741, 0.3064). Typical chromaticity distribution of a color region is shown in Fig.6 (a) and (b). The area painted in white in Fig.6 (a) is a part of a red region, where there are 2516 reliable pixels. The chromaticity distribution of the region is also painted in white in Fig.6 (b). The *ratio* ($=\sigma_1/\sigma_2$) of the region is 6.52, and its linear shape can be clearly observed.

Though the correct chromaticity of D65 illuminant is (x,y)=(0.3127, 0.3290), camera characteristics are related to the color reproduction. The comparison with the chromaticity of the neutral gray (N7) on the inner surface of the booth is more appropriate. Assuming that the image data is generated in sRGB space, the mean chroma-ticity of the gray background of the image in Fig.5 (a) was (0.283, 0,312). The chromaticity estimation error was about -0.009 in x direction and -0.006 in y direction.

The same scene was also taken under the illuminant A simulator (Condition 2 - Fig.7(a)). The image looks very yellowish. The same processing as above was applied, and Fig.7 (b) shows the estimation result. In this case, the estimated chromaticity was (x_2,y_2)=(0.4775, 0.4158). The mean chromaticity of the gray background in this image was (0.448, 0.415). The estimation error was about +0.027 in x direction and +0.001 in y direction. The estimation for the scene was successful, and the estimation error was reasonably small, though the estimation of x for Condition 2 was not so accurate.

However, the scene consists of plastic objects, whose reflection is ideally composed of diffuse reflection and specular reflection. We applied the algorithm to another scene, which contains only 'Gretag-Macbeth Color Checker®' under Condition 1. The surface of the colored areas is very matt, and no specular reflection can be observed (Fig. 8(a)). The same image processing as to the previous image (Fig. 5) was applied. As the Color Checker is flat and matt, each color region on the Color Checker was clearly divided as one color region after the color space division (Fig. 8(b)). The whole color space was divided into 30 subspaces. After the connected component labeling, the original image was divided into 6064 color regions. Figure 8(c) shows the chromaticity distribution of reliable pixels, and Fig. 8(d) shows the first principal axes and the estimated illumination chromaticity.

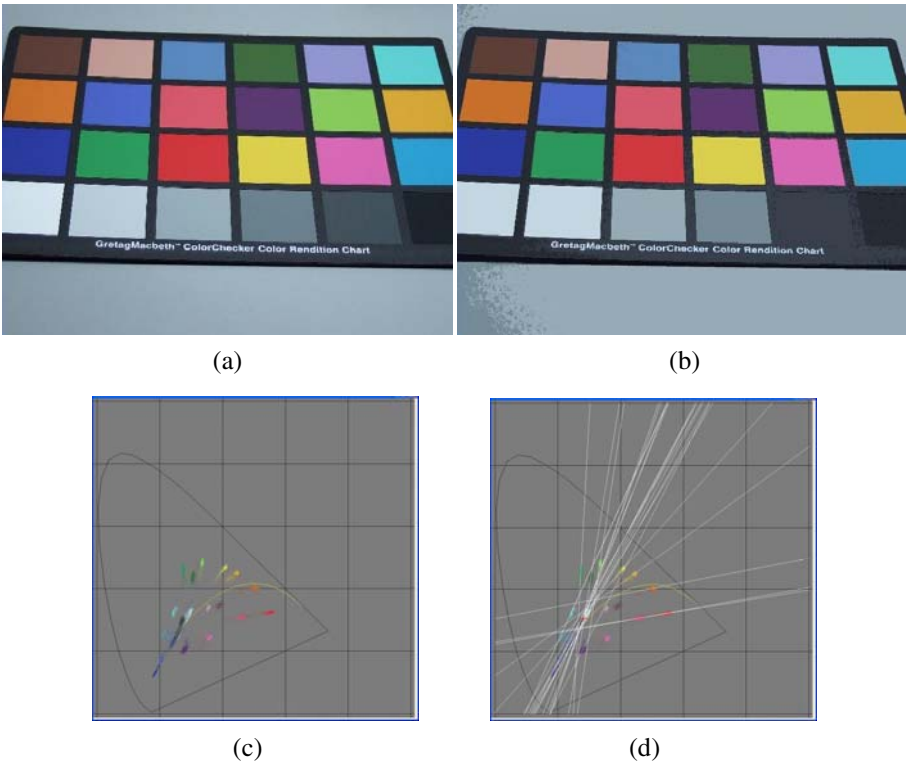

Fig. 8. Experiment on an image with matt objects. (a) Original image. (b) Color region image (30 colors). (c) Chromaticity distribution of reliable pixels. (d) Illumination chromaticity estimation.

Very interestingly, the color distribution of the pixels in each large color region, which corresponds to one color area on the Color Checker, is sufficiently elliptical and can be used for the illumination chromaticity estimation. The estimation result was (x_1,y_1)=(0.2810, 0.3069). The mean chromaticity of the gray background, in this case, was (0.286, 0.312). The chromaticity estimation error was about -0.005 in both x and y directions. The same scene was also taken under Condition 2, and the estimation was carried out. In this case, the estimated chromaticity was (x_2,y_2)=(0.4169, 0.4125). The estimation error was about -0.034 in x direction and -0.001 in y direction.

4.2 Discussion

In the previous subsection, it was shown that the illumination chromaticity estimation algorithm based on the two-dimensional DRM and the color space division is applicable to real images. One image contained typical objects with diffuse reflection and specular reflection, while another image contained objects with very matt surfaces. The estimation algorithm worked very well not only for the former image which has ideal characteristics for the algorithm, but also for the latter image without apparent specular reflection. In the real world, object surfaces would have the reflection characteristics between these two. The estimation algorithm can be applicable to most surfaces in real scenes.

The estimation result was sufficiently good for the images under Condition 1 (illuminant D65 simulator). However, it was not for the images under Condition 2 (illuminant A simulator). Under Condition 2, x coordinate estimation was especially inaccurate. The reason is not clear at this moment. Though more experiments should be carried out for the analysis and the algorithm improvement, it may be partly due to the fact that the camera used was one for consumer use. Color calibration may not be accurate, or some color rendering process may have been applied to the original signal. In addition, it may be due to the chromaticity distribution under Condition 2. From Fig. 7(b), it is observed that chromaticity distribution is pushed to upper area of the chromaticity diagram. Major first principal axes are oriented nearly parallel. This may cause the inaccuracy, especially in x direction.

5 Conclusions

In this paper, the illumination chromaticity estimation using the two-dimensional DRM combined with imperfect image segmentation was proposed. Though the color space division algorithm may divide a large homogeneous color region into several small regions or merge several color regions, the robust chromaticity estimation could find the illumination chromaticity based on the least squares method, allowing segmentation error to a certain extent. Wide dynamic range color regions that include both diffuse reflection and specular reflection areas were not necessary. The proposed algorithm was applied to real images taken by a digital camera. The result was encouraging. In addition, it turned out that the two-dimensional DRM is also applicable to apparently matt surfaces like Gretag-Macbeth Color Checker.

The scenes used for this experiment included many colors. The algorithm is considered to be useful for the scenes with a few colors, in principle. However, no algorithm is all-round for all images. In practice, combining the algorithm with other simpler methods (e.g. MOR or GWA) would be desirable.

Acknowledgement

This work was partly supported by KAKENHI 20500160.

References

1. Finlayson, G.D., Hubel, P.M., Hordley, S.: Color by Correlation. In: Proc. 5th Color Imaging Conference, pp. 6–11 (1997)
2. Barnard, K., Cardei, V., Funt, B.: A Comparison of Computational Color Constancy Algorithms – Part I & II. IEEE Trans. on Image Processing 1(9), 972–996 (2002)
3. Funt, B., Xiong, W.: Estimating Illumination Chromaticity via Support Vector Regression. In: Proc. 12th Color Imaging Conference, pp. 47–52 (2004)
4. Shafer, S.A.: Using Color to Separate Reflection Components. Color Res. Appl. 10, 210–218 (1985)
5. Tominaga, S.: Surface Identification Using the Dichromatic Reflection Model. IEEE Trans. PAMI-13, 658–670 (1991)

6. Saito, T.: Method and Apparatus for Illumination Color Measurement of a Color Image. Japanese Patent 2081885 (1988) (in Japanese)
7. Tominaga, S.: Consideration on a Color Reflection Model for Object Surfaces. IPSJ, 1988-CVIM-059 (1989) (in Japanese)
8. Saito, T.: Method and Apparatus for Illumination Chromaticity Measurement of a Color Image. Japanese Patent 2508237 (1989) (in Japanese)
9. Lehmann, T.M., Palm, C.: Color Line Search for Illuminant Estimation in Real-World Scenes. J. Opt. Soc. Am. A 18(11), 2679–2691 (2001)
10. Finlayson, G.D., Schaefer, G.: Solving for Colour Constancy using a Constrained Dichromatic Reflection Model. IJCV 42(3), 127–144 (2001)
11. Ebner, M., Herrmann, C.: On Determining the Color of the Illuminant Using the Dichromatic Reflection Model. In: Kropatsch, W.G., Sablatnig, R., Hanbury, A. (eds.) DAGM 2005. LNCS, vol. 3663, pp. 1–8. Springer, Heidelberg (2005)
12. Tajima, J., Ikeda, T.: High Quality Color Image Quantization, Utilizing Human Vision Characteristics. J. IIEEJ, 293–301 (1989) (in Japanese)
13. Ohtsu, N.: A Threshold Selection Method from Gray-Level Histograms. IEEE Trans. SMC-9(1), 62–66 (1979)